Australasian Physical & Engineering Sciences in Medicine (2019) 42:803–810
https://doi.org/10.1007/s13246-019-00784-z

SCIENTIFIC PAPER

Optimizing image quality using automatic exposure control based on the signal-difference-to-noise ratio: a phantom study

Hiroki Kawashima[1] · Katsuhiro Ichikawa[1] · Shinsuke Hanaoka[2] · Kosuke Matsubara[1]

Received: 13 June 2019 / Revised: 25 July 2019 / Accepted: 26 July 2019 / Published online: 8 August 2019

Abstract

This study proposes to adjust the sensitivity of automatic exposure control (AEC) for achieving consistent image quality over a range of subject thicknesses in abdominal radiography simulations. The relation between image quality and subject thickness was investigated using a digital radiography system with 10-, 15-, 20-, and 25-cm-thick acrylic phantom. Simple pixel signal-to-noise ratio (SNR) was measured to check the default AEC accuracy for each thickness, and image quality was evaluated using the signal-difference-to-noise ratio (SDNR) with an additional acrylic plate and bone-equivalent material. Based on the figure of merit theory, dose ratios to obtain constant image quality regardless of the subject thickness were calculated from SDNR results. The AEC setup was manually modified using this dose ratio, and visibility was examined using a CDRAD 2.0 contrast-detail analysis phantom. Moreover, the entrance surface dose (ESD) was estimated as an index of exposure dose using exposure parameters. The default AEC setup provided a constant simple pixel SNR for each subject thickness with a high accuracy. SDNRs decreased with an increase in the subject thickness. The calculated dose ratios relative to the results for 20 cm thickness were 0.424, 0.647, and 1.43 for 10, 15 and 25 cm, respectively, and a > 25% decrease in ESD was observed for smaller patients. CDRAD analysis using the modified AEC setup showed almost identical visibility for each thickness. Adjusting the sensitivity of AEC according to subject thickness can contribute toward the optimization of the exposure condition.

Keywords Digital radiography · Automatic exposure control · Image quality · Optimization · Entrance surface dose

Introduction

General radiography performed using a film screen system employs automatic exposure control (AEC), especially with a photo timer, to maintain constant optical density, regardless of the thickness of the patient's body. This technique is still in routine use, despite the current predominance of digital radiography (DR). Optimizing the exposure conditions using the AEC system is beneficial for providing stable image quality [1–3]. AEC systems measure the detector entrance dose to provide consistent reproducible exposures across a wide range of patient body sizes. Since the signal level of an image is linked to the noise levels in a linearized system, it is anticipated that the AEC system yields images with consistent noise levels. However, the subject contrast varies between patients with different body sizes, and the AEC system used in DR does not consider this variation in contrast.

Generally, the most relevant image quality evaluation measure for DR is the signal-difference-to-noise ratio (SDNR) [4, 5], which comprehensively evaluates the contrast and noise to assess the inherent physical image quality. This index plays an important role in optimizing exposure condition in digital imaging where the contrast no longer depends on the exposure dose level.

✉ Hiroki Kawashima
kawa3@med.kanazawa-u.ac.jp

Katsuhiro Ichikawa
ichikawa@mhs.mp.kanazawa-u.ac.jp

Shinsuke Hanaoka
hana43210@gmail.com

Kosuke Matsubara
matsuk@mhs.mp.kanazawa-u.ac.jp

[1] Faculty of Health Sciences, Institute of Medical, Pharmaceutical and Health Sciences, Kanazawa University, 5-11-80 Kodatsuno, Kanazawa 920-0942, Japan

[2] Radiology Division, Kanazawa University Hospital, 13-1 Takara-machi, Kanazawa 920-8641, Japan

Chest and abdominal radiography are frequently performed, and in most cases, the radiation dose is controlled by the AEC. Abdominal radiography, in particular, requires a relatively high entrance surface dose (ESD), which is approximately ten times higher than that required for chest radiography [6]. Since the abdominal organs overlap each other in a complex way, image quality requires the assessment of gas and soft tissue with low contrast. Therefore, an AEC technique that resulting in a constant SDNR would provide optimal dose across different patient thicknesses while maintaining the image quality required in clinical images. The dose adjustments required for this technique will be able to estimate by the calculation based on the figure of merit theory. It has been reported that the image quality of other modalities, such as computed tomography (CT) and mammography, could be improved by adjusting the sensitivity of the AEC as a function of the patient thickness [7–10]. However, to the best of our knowledge, few studies have evaluated the feasibility for DR.

The aim of this phantom study was to investigate the relation between the default AEC setup and image quality over a range of subject thickness assuming abdominal radiography and to propose the dose adjustment for achieving a consistent SDNR regardless of the subject thickness.

Methods

DR system and phantom

DR system used was an X-ray unit (RADspeed Pro, Shimadzu, Kyoto, Japan) with inherent filtration 2.8 mm Al and indirect-type CsI detector (Calneo HC, Japan Fujifilm, Kanagawa, Japan) with a 0.15-mm pixel pitch. Phantom images were acquired using a stationary anti-scatter grid (ratio, 10:1; density, 40 lines/cm; aluminium interspace material; and focus to grid distance, 150 cm), and linearized original data, to which only the grid pattern removal processing provided by the vendor was applied, were used for measurements. Linearity was checked according to the method specified in IEC 62220–1-1 [11].

Four acrylic thicknesses were used to assess the image quality as a function of subject size. An acrylic phantom made from 35×35 cm^2 slabs was used, which could be adjusted to thicknesses of 10, 15, 20, and 25 cm. The subject thickness of the average adult was determined to be 20 cm by referring to the Japan diagnostic reference levels (DRLs) 2015 [6]. Figure 1a shows the experimental geometry for measuring SDNR. A tube voltage of 80 kV was used without additional filters. Additionally, to compare the SDNR values, the lower tube voltages of 60 and 70 kV

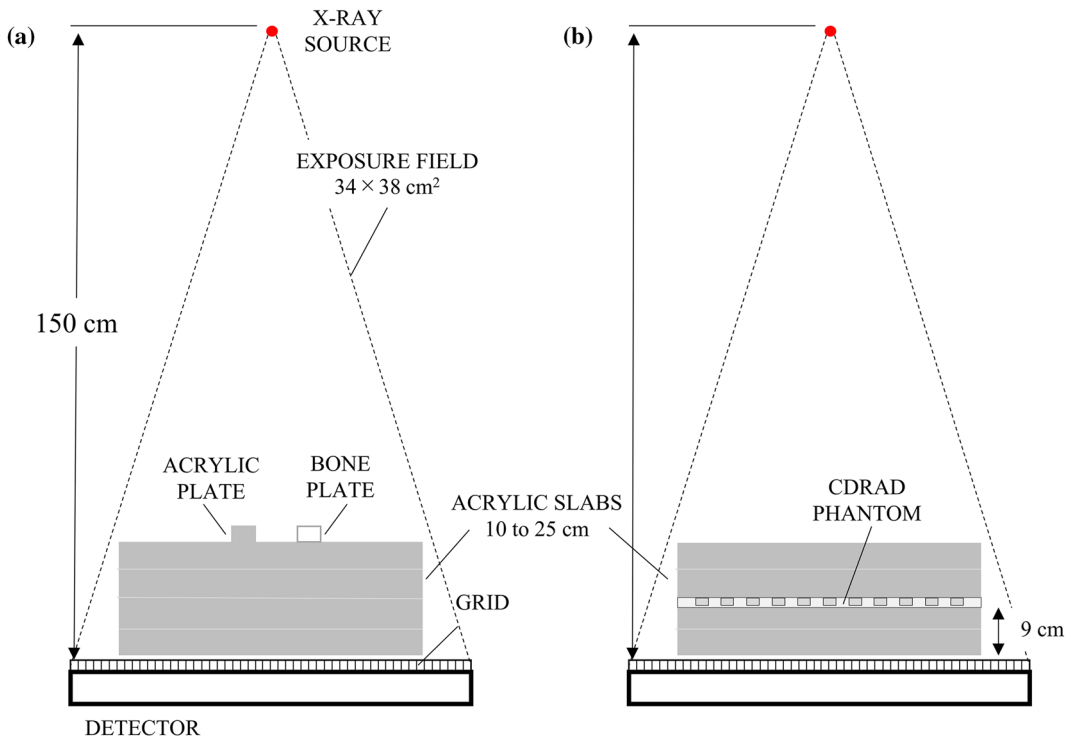

Fig. 1 Experiment geometry for the image quality measurements. **a** Signal-difference-to-noise ratio. Acrylic and bone plate were used as contrast objects, with both plates placed on top of the acrylic slabs. **b** Low-contrast visibility with a 1.0-cm-thick CDRAD phantom. The phantom was placed on top of the 9-cm-acrylic slabs and additional slabs were added on top of the phantom

Table 1 HVL value and back scatter factor for each tube voltage used in this study

Subject thickness	Tube voltage (kV)	HVL (mmAl)	Back scatter factor
10 cm	60	2.25	1.32
	70	2.63	1.36
	80	2.94	1.39
15 cm	60	2.25	1.32
	70	2.63	1.36
	80	2.94	1.39
20 cm	80	2.94	1.39
25 cm	80	2.94	1.39
	90	3.20	1.41
	100	3.53	1.43

were tested for subjects with 10 and 15 cm thickness, and the higher tube voltages of 90 and 100 kV for subjects with 25 cm thickness because the operator tends to change the tube voltage depending on subject thickness in clinical practice. These radiation qualities are listed in Table 1. The source-to-image distance was 150 cm with 7.3 cm air gap between subject and image receptor, and the radiation field was set to 34×38 cm^2, which is set in accordance with the size used in clinical practice; it was slightly larger than acrylic phantom used in this study.

Image quality evaluation

SDNR is known as the most relevant image quality indicator in DR, and several optimization studies have used this index [2, 5, 12–15]. A digital image with a higher level of SDNR could inherently provide superior image quality [4]. Herein, for the SDNR measurement, an additional acrylic plate and plate made of a bone-equivalent material (density, 1.73 cm^3/g; product code 4120–220 BE-H-10, manufactured by Kyoto Kagaku, Kyoto Japan), both 2×2 cm^2 and 1-cm thick, were placed on each thickness of acrylic phantom as shown in Fig. 1a. These contrasts were corresponding to soft-tissues and bones observed in abdominal radiographs. Square region of interests (ROIs) of 10×10 mm^2 were placed at the two plates and on the background between the two plates to measure the mean pixel values and standard deviations.

A mean pixel value of back ground (S_B) and simple pixel signal-to-noise ratio (SNR) was calculated to investigate the characteristics of the default AEC. Dividing S_B by the standard deviation of background (σ_B) gave the simple pixel SNR. Then, SDNR was obtained to compare the comprehensive image quality and to estimate dose ratios between the default and modified AEC setup. It can be calculated as the ratio of object to background signal difference ($S_B - S_M$) to the standard deviation of background (σ_B) [15, 16]. $SDNR_{acryl}$ and $SDNR_{bone}$ were measured from mean pixel values of additional acrylic and bone plates, respectively.

AEC settings

Image data using default AEC setup were obtained with the combination of each subject thickness and tube voltages. For the proposed method, we changed the mAs values to obtain the equivalent SDNR in each subject thickness. Image noise (standard deviation) used in the calculation of SDNR is governed by Poisson statistics, also contrast is not affected by the dose in most cases. Therefore, $SDNR^2$ is proportional to the dose. Hence, dose ratios for adjusting the mAs value were calculated using this relationship (figure of merit theory) to scale mAs selected for the default AEC, to estimate mAs value required for the AEC configured to deliver constant SDNR [4, 5]. Herein, the SDNR result of the 20-cm thick set a target figure and ratio to each subject thickness was obtained. This calculation was only tested for 80-kV results. The contrast object used for the SDNR calculation was an acrylic plate since it is often more important in abdominal radiography for evaluating soft tissues rather than the bone structure. The dose ratio was multiplied by the mAs value when using the default AEC, and the resulting value was then defined as the modified AEC setup. However, in this feasibility study, it was difficult to tune the sensitivity of the AEC setup automatically; therefore, the mAs values were adjusted manually to the closest value that can be set.

CDRAD analysis

The image visibility and quality in condition close to clinical use were evaluated using a 1.0-cm-thick CDRAD 2.0 contrast-detail analysis phantom (Artinis Medical Systems, Einsteinweg, The Netherlands) [17]; the depth and diameters of the holes ranged from 0.3 to 8.0 mm. The X-ray image will show 225 squares arranged in 15 columns and 15 rows. The phantom was positioned on top of the 9-cm acrylic slabs and additional slabs were then added on top of the phantom as shown in Fig. 1b. The phantom images were obtained eight times for each subject size using the default and modified AEC setups with a tube voltage of 80 kV. The analyzed image dataset was in the DICOM format, and default image processing for abdominal radiographs was performed based on the manufacturer's protocols. Automatic scoring was performed using a software (CDRAD Analyzer, version 2.1; Artinis Medical Systems), and contrast-detail curves were calculated. The inverse image quality figure (IQF_{inv}) was calculated from the curves as follows [18]:

$$IQF_{inv} = \frac{100}{\sum_{i=1}^{15} C_i D_{i,th}}, \quad (1)$$

where $D_{i,th}$ denotes the threshold diameter in contrast column i and C_i is the correctly identified contrast values. The

summation is over all the columns (n = 15). Higher IQF_{inv} values indicate a better low-contrast visibility. IQF_{inv} values were calculated for all the eight analyzed images and the results were averaged for each condition. Differences in IQF_{inv} between different subject thickness for each AEC setup were evaluated statistically with a one-way analysis variance (ANOVA), followed by post hoc tests with the Bonferroni correction performed using BellCurve for Excel statistical software (Social Survey Research Information Co., Ltd. Tokyo Japan). For variations in the low contrast visibility with thickness, ANOVA p values of less than 0.05 are considered to be statistically significant. When the ANOVA yields nonsignificant results, no further test is needed. On the contrary, when the ANOVA was significant, post hoc tests were conducted.

Entrance surface dose

In this study, ESD was used as an indicator of exposure dose used in the Japan DRLs 2015 [6]. ESD was measured using exposure parameters related to a 6-cm^3 general purpose ionization chamber (Model 20X6-6; Radcal, Monrovia, CA, USA). The chamber was located 80 cm from the X-ray focal spot, and the acrylic phantom was removed when measuring the dose. The exposure dose was measured at a constant tube current–time product of 20 mAs. Values of ESD per unit mAs were calculated to obtain the required mAs values; these were combined with the backscatter factors (Table 1) corresponding to the radiation qualities (the half-value layer) and radiation field and the distance factors based on the inverse square theorem [19].

Results

Figure 2 shows the results of background mean pixel values (Fig. 2a) and simple pixel SNRs (Fig. 2b) for each tube voltage setting using the default AEC setup. In particular, the results of 80 kV were almost identical for each subject thickness.

Figure 3a shows $SDNR^2$ results obtained using the default AEC with a tube voltage of 80 kV for each subject thickness. Y-axis indicates the relative value to 20-cm subject thickness. $SDNR^2$s decreased with an increase in the subject thickness. Figure 3b shows the dose ratios for equivalent image quality calculated from the $SDNR^2$ value results with the acrylic contrast. A quadratic regression curve showed a close fit to the data points. The mAs value for the modified AEC setup was calculated by multiplying the dose ratio by the mAs value obtained with the default AEC setup. Based on these ratios, the mAs values for the modified AEC setup were 2.40 to 1.02 mAs, 6.80 to 4.40 mAs, and 44.7 to 63.8 mAs for the 10, 15 and 25 cm acrylic thicknesses, respectively.

Figure 4 shows the SDNR results as a function of ESD for each tube voltage settings. Results of acrylic (Fig. 4a) and bone contrast (Fig. 4b) showed similar trends. SDNRs also decreased with an increase in the subject thickness except for the modified AEC setup. The use of lower tube voltage at a thinner subject thickness improved SDNR (9.9–29%), but the ESD also increased (45–107%). The use of higher tube voltage at thicker subject thickness decreased SDNR (1.0–21%) and ESD (25–39%). After adjusting the mAs values, SDNR results were almost identical for each subject thickness within 3% of each other. From the viewpoint of ESD, the dose reductions in comparison with the default setup were 47.9% and 26.5% for the thicknesses of 10 and

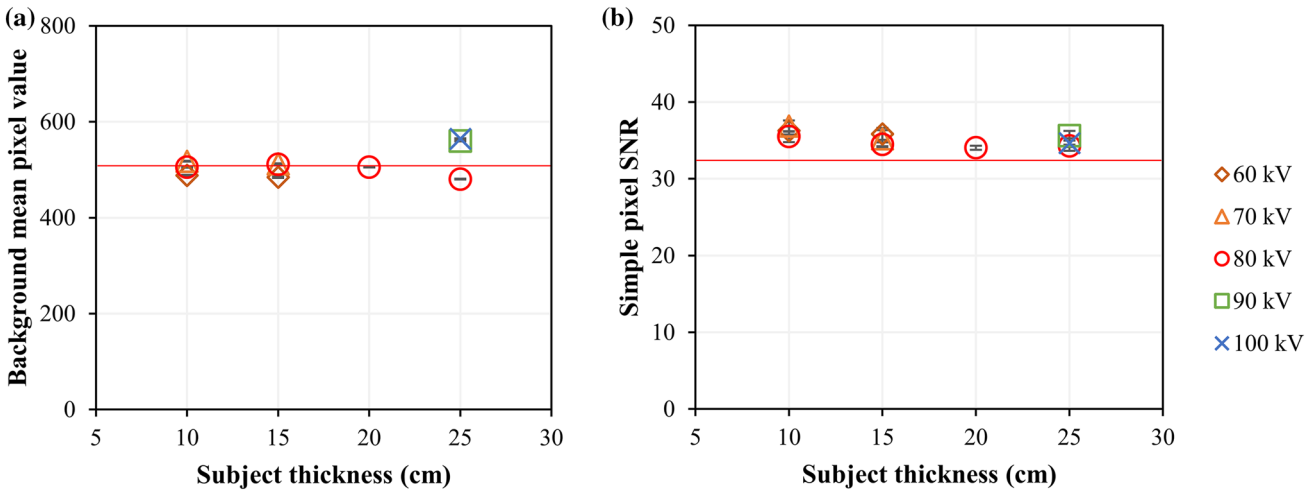

Fig. 2 Results of background mean pixel values and simple pixel SNRs for each tube voltage setting using the default AEC setup. Red line shows the reference value i.e., the results of subject thickness of 20 cm with 80 kV

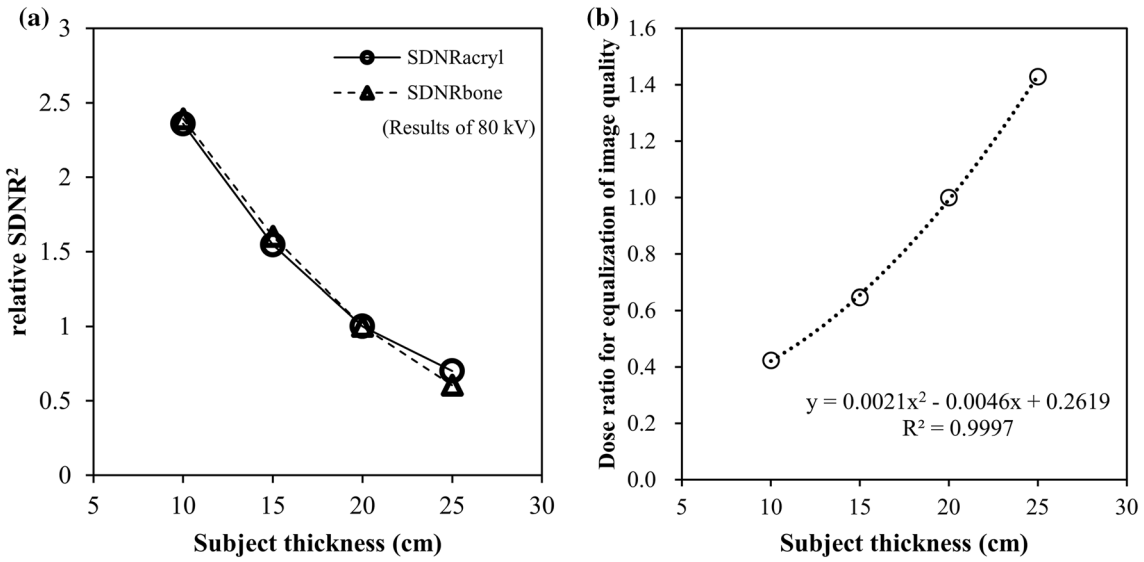

Fig. 3 **a** Relative $SDNR^2$ result values for acrylic and bone contrast when using the default automatic exposure control setup. **b** Graph showing the dose ratios for the equalization of image quality for the four subject thicknesses. The data points were well fitted by a quadratic function

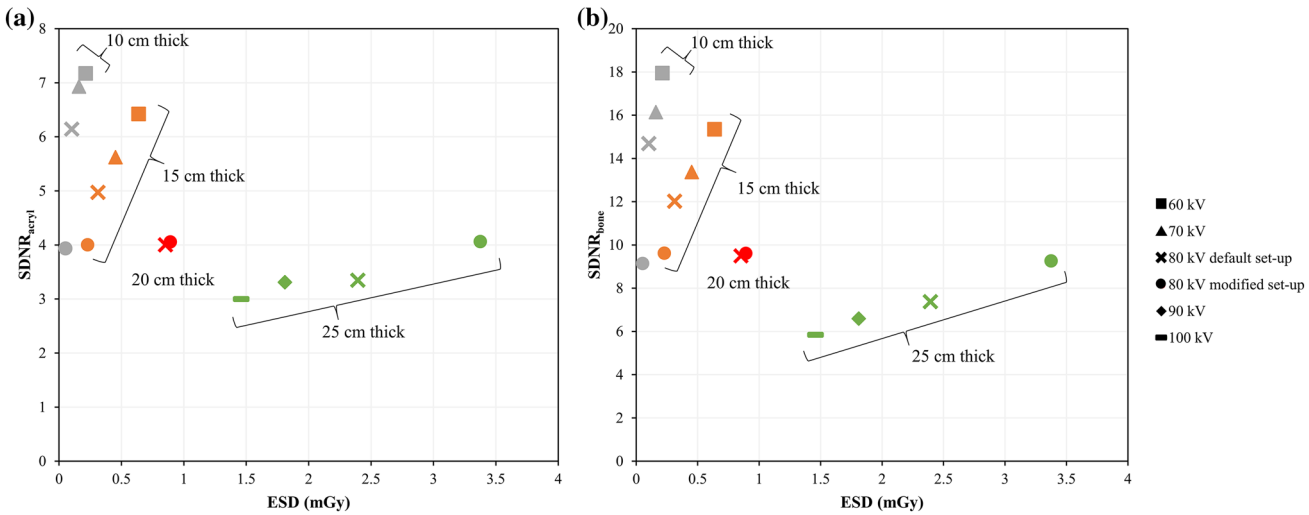

Fig. 4 SDNR results for **a** acrylic and **b** bone contrast as a function of ESD. Grey, orange, red and green colour shows the results for 10, 15, 20, and 25 cm, respectively. Default setup results are widely plotted from higher image quality, lower dose value to lower image quality, higher dose value. On the contrary, the modified setup results are plotted on horizontal band; it shows similar SDNR values

15 cm, respectively. On the contrary, the ESD for 25 cm increased by 41%.

Figure 5 shows the CDRAD analysis results. In the contrast-detail curves for the default AEC, the low-contrast visibility depended on the subject thickness (Fig. 5a). The IQF_{inv} values for the default AEC decreased with an increase in the subject thickness, which is similar to SDNR results (Fig. 5b). The ANOVA analysis was significant [$F(3,28) = 144$, $p < 0.001$], and the post hoc test showed significant results for all the subjects thickness ($p < 0.001$). After the dose adjustment, the contrast-detail curves for modified AEC were almost identical, regardless of subject thickness; there was no significant difference by one-way ANOVA among the IQF_{inv} values for the four subject thicknesses [$F(3,28) = 0.79$, $p = 0.509$; Fig. 5c].

Figure 6 shows the enlarged images of the CDRAD phantom part for the default and modified AEC setups. The window conditions for the five images were adjusted based on the ROI measurements at the drilled holes and background. Similar to SDNR and CDRAD analyses results, the image noise differed with subject thickness when using the default AEC, whereas the images showed

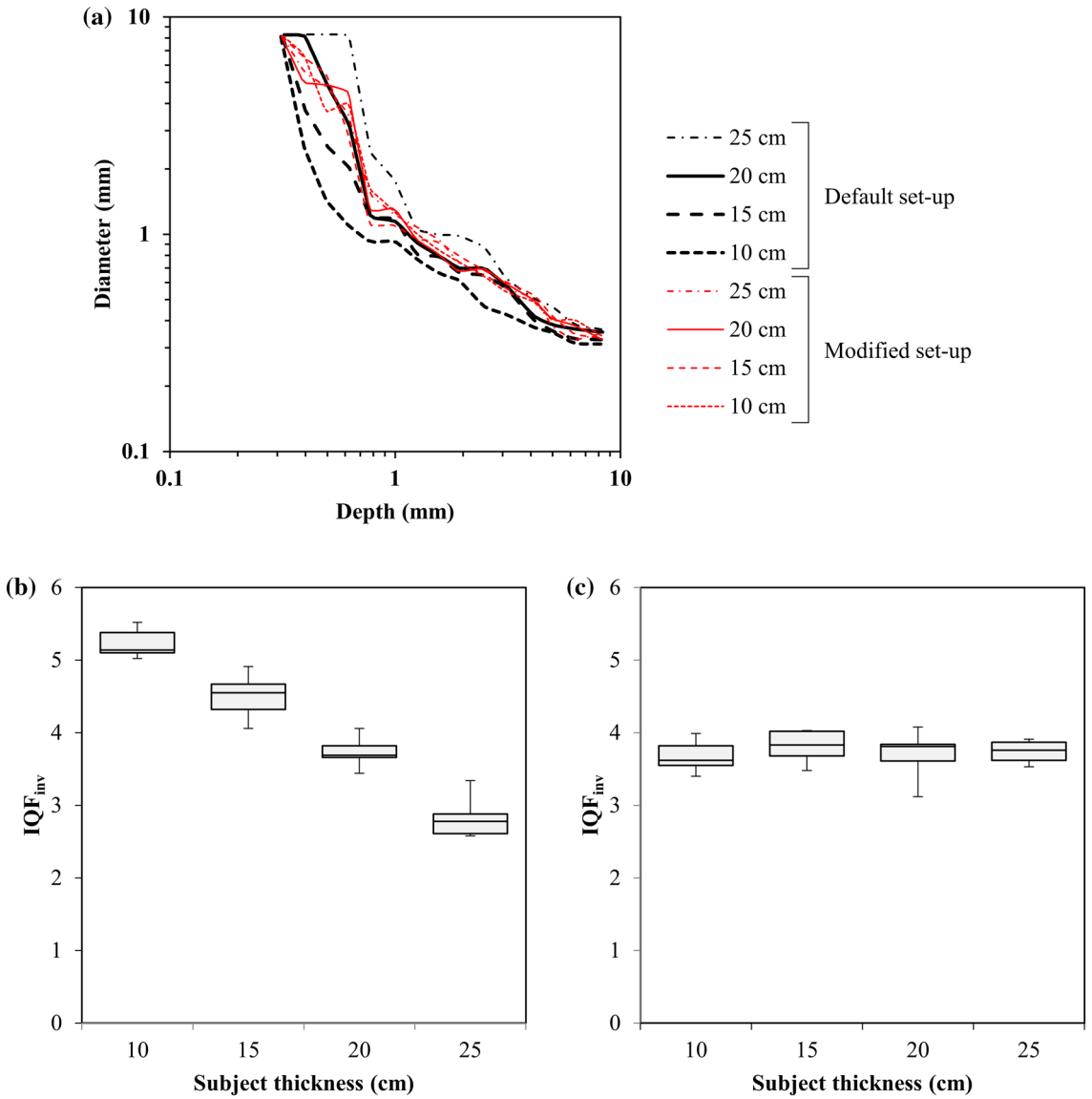

Fig. 5 CDRAD analysis results. **a** The graph shows the average contrast-detail curves for each subject thickness with the default (black line) and modified AEC setup (red line). **b** Box plots show the results of IQFinv for (b) default and **c** modified AEC after adjustment

nearly identical noise to the reference image when using the modified AEC after the dose adjustment.

Discussion

This study proposes an adjustment to AEC sensitivity that results in constant SDNR values regardless of subject thickness. Using the default AEC setup with a tube voltage of 80 kV provided a constant signal level. Errors due to different subject thickness were a concern; however, the detector entrance dose was controlled with high precision regardless of subject thickness [2]. However, considering the image quality, the contrast variation due to different subject thicknesses caused by the differences in scatter fraction and radiation quality, was not considered in the control regulation. The SDNR evaluation showed that images of patients with a small body size were superior in quality; in other words, the smaller patients were receiving higher than required radiation dose. On the contrary, the image quality for patients with a large body size was degraded, indicating an insufficient dose. Additionally, we found that the changing the tube voltage depending on subject thickness caused an increase in dose or degraded image quality at the same AEC setting.

The proposed dose ratio based on the figure of merit calculation achieved a constant SDNR. Its effect was demonstrated by the CDRAD analysis. Use of the dose ratio resulted in an ESD reduction of approximately 25−48% for the small

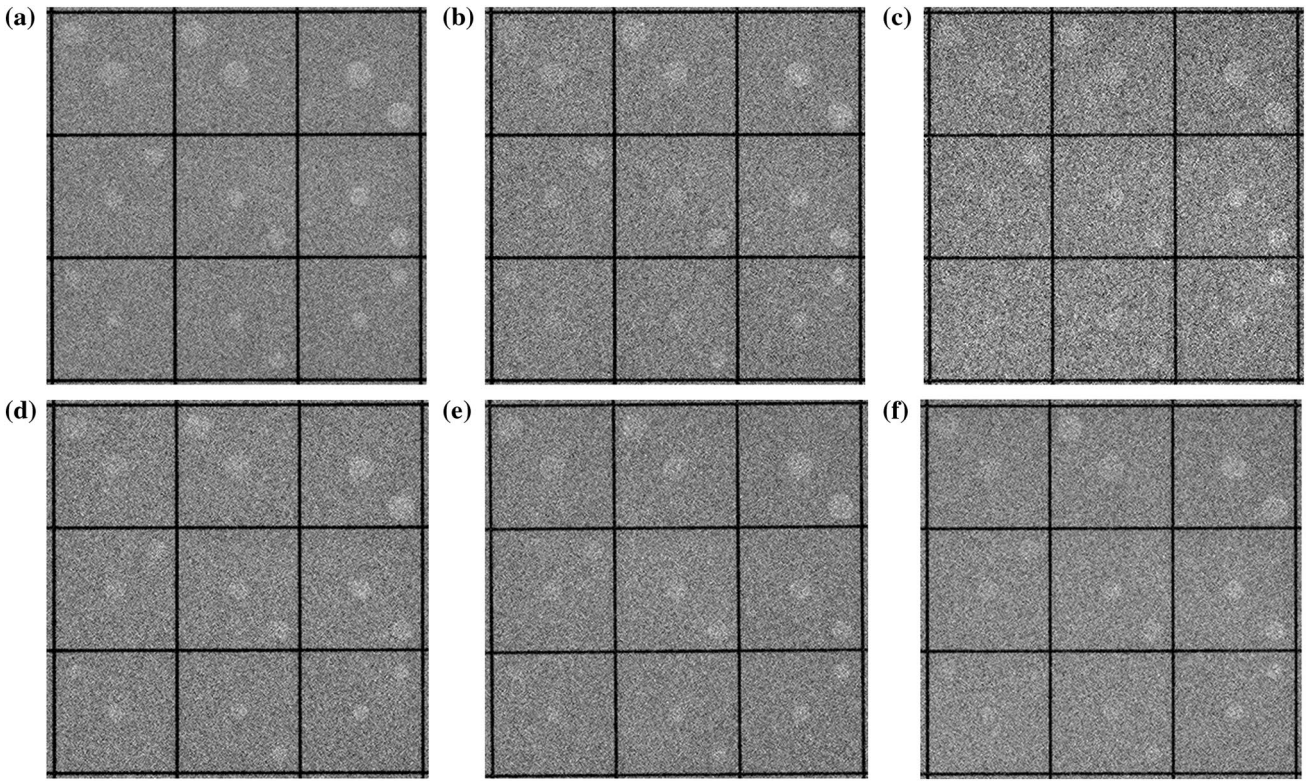

Fig. 6 Enlarged images of part of the CDRAD phantom. Subject thicknesses: **a** 15, **b** 20, and **c** 25 cm using default AEC; **d** 15, **e** 20 and **f** 25 cm using the modified AEC

patient size. A detailed study optimizing AEC in planer images for mammography has been reported [7]. Unlike the proposal in this study, the conclusion of that study was that a dose reduction for thin subjects (with compressed breast thickness of ≤ 40 mm) was unnecessary because the doses were below the achievable level of the guideline; therefore, the dose reduction would lead to a reduction in detectability [20]. It is likely that the signals targeted in the examination differ between DR and mammography, and breast imaging requires the visualization of finer structures. On the contrary, it has been proposed that constant CNR, regardless of radiation qualities, is useful for both computed radiography and DR [2]; however, to the best of our knowledge, no previous study was focused on subject thickness.

A possible concern of the method proposed herein is that the ESD would increase more for patients with a large body size, though it can be considered that such patients require that dose. The standard body size, according to Japan DRLs 2015, was defined as 20-cm thick for abdominal radiography. For this body size, the ESD was < 1.0 mGy using the default AEC setup in this study; however, the ESD is set as 3.0 mGy in the DRL, wherein the data were mainly investigated by computed radiography. Recent flat panel detector systems have higher detective quantum efficiency than that of computed radiography [21]; therefore, the exposure dose can be reduced even when the modified AEC setup is used for large patients. In addition, it is possible that image quality can be improved by varying the image processing according to subject thickness. Various edge-preserving noise reduction filters have been studied in the past, and it may be effective to apply them [22, 23].

This study has some limitations that should be acknowledged. First, we evaluated the effect of different tube voltages but grid-less imaging in small patients and additional metal filtration were not investigated in this study. Second, our key idea exceeds the capability of current AEC technology for abdominal radiography. The dose ratio for equalizing SDNR presupposed that the subject thickness could be estimated before or during the examination. The AEC system for CT can adjust radiation dose using scout images [8, 9], and in mammography, it is possible to estimate the attenuation from the height of a compression paddle and to "pre expose" for AEC [24]. For the DR system, it seems to be difficult to estimate subject thickness instantaneously at the time of the imaging and to feed this back to the AEC control system in the current system. We believe that one of the method to overcome this issue is to use a three-dimensional camera for the estimation [25]. Thereby, it might be possible to optimize the setting of AEC for each region of the body by using our proposed method, though we targeted

only abdomen in this study. Such new technical developments are expected in the future.

Conclusion

Default AEC setup provided constant pixel values with high accuracy, regardless of subject thickness. On the contrary, this indicated that the image quality for the different thicknesses was notably different because of contrast variation. Therefore, a dose ratio as a function of subject thickness was proposed to obtain constant SDNR values based on the figure of merit theory. A CDRAD analysis of the proposed modified AEC setup showed equivalent low-contrast visibility for the different subject thicknesses. Adjusting the sensitivity of AEC according to subject thickness can be contributed to optimization of the exposure condition.

Compliance with ethical standards

Conflict of interest The authors declare no conflicts of interest associated with this manuscript.

Ethical approval This article does not contain any studies with human participants or animals performed by any of the authors.

References

1. Uffmann M, Schaefer-Prokop C (2009) Digital radiography: the balance between image quality and required radiation dose. Eur J Radiol 72(2):202–208
2. Marshall NW (2009) An examination of automatic exposure control regimes for two digital radiography systems. Phys Med Biol 54(15):4645–4670
3. Doyle P, Gentle D, Martin CJ (2005) Optimising automatic exposure control in computed radiography and the impact on patient dose. Radiat Prot Dosim 114(1–3):236–239
4. Samei E, Dobbins JT 3rd, Lo JY, Tornai MP (2005) A framework for optimising the radiographic technique in digital X-ray imaging. Radiat Prot Dosim 114(1–3):220–229
5. Kawashima H, Ichikawa K, Nagasou D, Hattori M (2017) X-ray dose reduction using additional copper filtration for abdominal digital radiography: evaluation using signal difference-to-noise ratio. Phys Med 34:65–71
6. Japan network for research and information on medical exposures (2015) Diagnostic reference levels based on latest surveys in japan -Japan DRLs 2015-. https://www.radher.jp/J-RIME/report/DRLhoukokusyoEng.pdf. Accessed Sept 2016
7. Salvagnini E, Bosmans H, Struelens L, Marshall NW (2015) Tailoring automatic exposure control toward constant detectability in digital mammography. Med Phys 42(7):3834–3847
8. Kalender WA, Buchenau S, Deak P, Kellermeier M, Langner O, van Straten M et al (2008) Technical approaches to the optimisation of CT. Phys Med 24(2):71–79
9. Funama Y, Sugaya Y, Miyazaki O, Utsunomiya D, Yamashita Y, Awai K (2013) Automatic exposure control at MDCT based on the contrast-to-noise ratio: theoretical background and phantom study. Phys Med 29(1):39–47
10. Kawashima H, Ichikawa K, Hanaoka S, Matsubara K, Takata T (2018) Relationship between size-specific dose estimates and image quality in computed tomography depending on patient size. J Appl Clin Med Phys 19(4):246–251
11. International Electrotechnical Commission (2015) Medical electrical equipment-characteristics of digital X-ray imaging devices - part 1–1: determination of the detective quantum efficiency-detectors used in radiographic imaging, IEC, Geneva, Switzerland, IEC 62220–1–1
12. Pavan ALM, Alves AFF, Duarte SB, Giacomini G, Sardenberg T, Miranda JRA et al (2015) Quality and dose optimization in hand computed radiography. Phys Med 31(8):1065–1069
13. Copple C, Robertson ID, Thrall DE, Samei E (2013) Evaluation of two objective methods to optimize kVp and personnel exposure using a digital indirect flat panel detector and simulated veterinary patients. Vet Radiol Ultrasound 54(1):9–16
14. Salvagnini E, Bosmans H, Struelens L, Marshall NW (2013) Effective detective quantum efficiency for two mammography systems: measurement and comparison against established metrics. Med Phys 40(10):101916
15. Aslund M, Cederström B, Lundqvist M, Danielsson M (2006) Scatter rejection in multislit digital mammography. Med Phys 33(4):933–940
16. Beutel J, Kundel HL, Van Metter RL (2000) Handbook of medical imaging, vol 1. SPIE, Bellingham, Wash, pp 79–159
17. De Crop A, Bacher K, Van Hoof T, Smeets PV, Smet BS, Vergauwen M et al (2012) Correlation of contrast-detail analysis and clinical image quality assessment in chest radiography with a human cadaver study. Radiology 262(1):298–304
18. Thijssen MAO, Bijkerk KR, van der Burght RJM (1998) Manual: contrast-detail phantom Artinis CDRADtype 2.0. St. Radboud, The Netherlands: ProjectQuality Assurance in Radiology, Department of Ra-diology, University Hospital Nijmegen
19. International Atomic Energy Agency (1983) Absorbed dose determination in photon and electron beams; an international code of practice. Technical Reports, Vienna, p 277
20. Perry N, Broeders M, de Wolf C, Törnberg N, Holland R, von Karasa L (2006) European protocol for the quality control of the physical and technical aspects of mammography screening, European guidelines for quality assurance in breast cancer screening and diagnosis, forth edition, European Commission, https://www.euref.org. Accessed Oct 2018
21. Rivetti S, Lanconelli N, Bertolini M, Nitrosi A, Burani A (2013) Characterization of a clinical unit for digital radiography based on irradiation side sampling technology. Med Phys 40(10):101902
22. Körner M, Weber CH, Wirth S, Pfeifer KJ, Reiser MF, Treitl M (2007) Advances in digital radiography: physical principles and system overview. Radiographics 27(3):675–686
23. Yamada S, Murase K (2005) Effectiveness of flexible noise control image processing for digital portal images using computed radiography. Br J Radiol 78(930):519–527
24. Williams MB, Raghunathan P, More MJ, Seibert JA, Kwan A, Lo JY (2008) Optimization of exposure parameters in full field digital mammography. Med Phys 35(6):2414–2423
25. Saltybaeva N, Schmidt B, Wimmer A, Flohr T, Alkadhi H (2018) Precise and automatic patient positioning in computed tomography. Invest Radiol 53(11):641–646